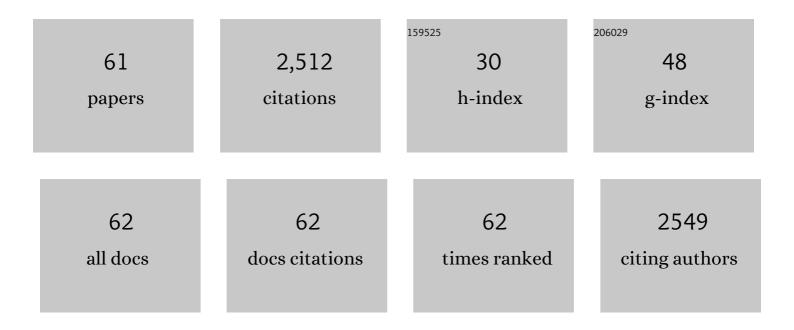
List of Publications by Year in descending order

Source: https://exaly.com/author-pdf/18494/publications.pdf Version: 2024-02-01



#	Article	IF	CITATIONS
1	Cement based electromagnetic shielding and absorbing building materials. Cement and Concrete Composites, 2006, 28, 468-474.	4.6	231
2	Biomass derived porous carbon (BPC) and their composites as lightweight and efficient microwave absorption materials. Composites Part B: Engineering, 2021, 207, 108562.	5.9	177
3	A facile hydrothermal synthesis of MnO ₂ nanorod–reduced graphene oxide nanocomposites possessing excellent microwave absorption properties. RSC Advances, 2015, 5, 88979-88988.	1.7	113
4	Microwave absorption performance of Ni(OH)2 decorating biomass carbon composites from Jackfruit peel. Applied Surface Science, 2018, 447, 261-268.	3.1	89
5	Investigation of the electromagnetic characteristics of cement based composites filled with EPS. Cement and Concrete Composites, 2007, 29, 49-54.	4.6	84
6	Biomass carbon derived from pine nut shells decorated with NiO nanoflakes for enhanced microwave absorption properties. RSC Advances, 2019, 9, 9126-9135.	1.7	73
7	Reduced graphene oxide (RGO)/Mn3O4 nanocomposites for dielectric loss properties and electromagnetic interference shielding effectiveness at high frequency. Ceramics International, 2016, 42, 936-942.	2.3	70
8	Construction of natural fiber/polyaniline core-shell heterostructures with tunable and excellent electromagnetic shielding capability via a facile secondary doping strategy. Composites Part A: Applied Science and Manufacturing, 2020, 137, 105994.	3.8	69
9	Synthesis and photocatalytic degradation of methylene blue over p-n junction Co3O4/ZnO core/shell nanorods. Materials Chemistry and Physics, 2015, 155, 1-8.	2.0	68
10	Facile synthesis of α-MnO2 nanorods at low temperature and their microwave absorption properties. Materials Chemistry and Physics, 2014, 143, 1061-1068.	2.0	62
11	Effective fabrication of flexible nickel chains/acrylate composite pressure-sensitive adhesives with layered structure for tunable electromagnetic interference shielding. Advanced Composites and Hybrid Materials, 2022, 5, 2906-2920.	9.9	61
12	Tuning the microwave absorption capacity of TiP2O7 by composited with biomass carbon. Applied Surface Science, 2020, 515, 145974.	3.1	59
13	Cu ₂ O templating strategy for the synthesis of octahedral Cu ₂ O@Mn(OH) ₂ core–shell hierarchical structures with a superior performance supercapacitor. Journal of Materials Chemistry A, 2018, 6, 13668-13675.	5.2	56
14	ZnO-Decorated In/Ga Oxide Nanotubes Derived from Bimetallic In/Ga MOFs for Fast Acetone Detection with High Sensitivity and Selectivity. ACS Applied Materials & amp; Interfaces, 2020, 12, 26161-26169.	4.0	54
15	Microwave absorption characteristics of manganese dioxide with different crystalline phase and nanostructures. Materials Chemistry and Physics, 2010, 124, 639-645.	2.0	53
16	Porous NiO nanosheets self-grown on alumina tube using a novel flash synthesis and their gas sensing properties. RSC Advances, 2015, 5, 4880-4885.	1.7	52
17	Enhanced microwave absorption properties of MnO2 hollow microspheres consisted of MnO2 nanoribbons synthesized by a facile hydrothermal method. Journal of Alloys and Compounds, 2016, 676, 224-230.	2.8	52
18	Jute-based porous biomass carbon composited by Fe3O4 nanoparticles as an excellent microwave absorber. Journal of Alloys and Compounds, 2019, 803, 1119-1126.	2.8	51

#	Article	IF	CITATIONS
19	Radio-wave electrical conductivity and absorption-dominant interaction with radio wave of exfoliated-graphite-based flexible graphite, with relevance to electromagnetic shielding and antennas. Carbon, 2020, 157, 549-562.	5.4	48
20	Morphology control of porous CuO by surfactant using combustion method. Applied Surface Science, 2015, 349, 844-848.	3.1	47
21	Binder-free NiO@MnO 2 core-shell electrode: Rod-like NiO core prepared through corrosion by oxalic acid and enhanced pseudocapacitance with sphere-like MnO 2 shell. Electrochimica Acta, 2016, 189, 83-92.	2.6	47
22	Self-grown MnO 2 nanosheets on carbon fiber paper as high-performance supercapacitors electrodes. Electrochimica Acta, 2016, 217, 16-23.	2.6	43
23	Effect of the planar coil and linear arrangements of continuous carbon fiber tow on the electromagnetic interference shielding effectiveness, with comparison of carbon fibers with and without nickel coating. Carbon, 2019, 152, 898-908.	5.4	43
24	Electromagnetic characteristics of nanometer manganese dioxide composite materials. Journal of Electronic Materials, 2006, 35, 892-896.	1.0	42
25	Enhanced microwave absorption of biomass carbon/nickel/polypyrrole (C/Ni/PPy) ternary composites through the synergistic effects. Journal of Alloys and Compounds, 2022, 890, 161887.	2.8	42
26	MOFs-derived NiFe2O4 fusiformis with highly selective response to xylene. Journal of Alloys and Compounds, 2019, 784, 102-110.	2.8	40
27	Carbon spheres@MnO2 core-shell nanocomposites with enhanced dielectric properties for electromagnetic shielding. Scientific Reports, 2017, 7, 15841.	1.6	38
28	A Discrete Slab Absorber: Absorption Efficiency and Theory Analysis. Journal of Composite Materials, 2006, 40, 1841-1851.	1.2	37
29	Effect of calcination temperatures on the electrochemical performances of nickel oxide/reduction graphene oxide (NiO/RGO) composites synthesized by hydrothermal method. Journal of Physics and Chemistry of Solids, 2016, 98, 209-219.	1.9	37
30	Effect of doping MnO2 on magnetic properties for M-type barium ferrite. Journal of Magnetism and Magnetic Materials, 2007, 311, 507-511.	1.0	36
31	Highly sensitive nonenzymatic H2O2 sensor based on NiFe-layered double hydroxides nanosheets grown on Ni foam. Surfaces and Interfaces, 2018, 12, 102-107.	1.5	32
32	Magnetic FeOX/biomass carbon composites with broadband microwave absorption properties. Journal of Alloys and Compounds, 2022, 903, 163894.	2.8	31
33	MOF-on-MOF nanoarchitecturing of Fe2O3@ZnFe2O4 radial-heterospindles towards multifaceted superiorities for acetone detection. Chemical Engineering Journal, 2022, 442, 136094.	6.6	31
34	Fe3O4/Fe/C composites prepared by a facile thermal decomposition method and their application as microwave absorbers. Journal of Alloys and Compounds, 2019, 784, 1123-1129.	2.8	30
35	Frequency and temperature effects on dielectric and electrical characteristics of α-MnO2 nanorods. Powder Technology, 2012, 224, 356-359.	2.1	28
36	Highly Sensitive and Selective Toluene Sensor of Bimetallic Ni/Fe-MOFs Derived Porous NiFe ₂ O ₄ Nanorods. Industrial & Engineering Chemistry Research, 2019, 58, 9450-9457.	1.8	27

#	Article	IF	CITATIONS
37	Preparation and electromagnetic shielding effectiveness of cobalt ferrite nanoparticles/carbon nanotubes composites. Nanomaterials and Nanotechnology, 2019, 9, 184798041983782.	1.2	26
38	Combustion synthesized hierarchically porous WO3 for selective acetone sensing. Materials Chemistry and Physics, 2016, 184, 155-161.	2.0	25
39	MOFs-Derived Porous NiFe2O4 Nano-Octahedrons with Hollow Interiors for an Excellent Toluene Gas Sensor. Nanomaterials, 2019, 9, 1059.	1.9	25
40	Hydrothermal synthesis of Co3O4 nanorods on nickel foil. Materials Letters, 2014, 123, 187-190.	1.3	22
41	Expanded Polystyrene as an Admixture in Cement-Based Composites for Electromagnetic Absorbing. Journal of Materials Engineering and Performance, 2007, 16, 68-72.	1.2	21
42	Temperature dependent dielectric characterization of manganese dioxide nanostructures with different morphologies at low frequency. Journal of Alloys and Compounds, 2010, 507, 126-132.	2.8	20
43	Facile synthesis of core–shell carbon nanotubes@MnOOH nanocomposites with remarkable dielectric loss and electromagnetic shielding properties. RSC Advances, 2016, 6, 90002-90009.	1.7	20
44	RGO/KMn8O16 composite as supercapacitor electrode with high specific capacitance. Ceramics International, 2016, 42, 5195-5202.	2.3	19
45	Synthesis of core-shell carbon sphere@nickel oxide composites and their application for supercapacitors. Ionics, 2018, 24, 513-521.	1.2	19
46	A novel microwave absorption material of Ni doped cryptomelane type manganese oxides. Ceramics International, 2015, 41, 5688-5695.	2.3	16
47	Absorption-dominant radio-wave attenuation loss of metals and graphite. Journal of Materials Science, 2021, 56, 8037-8047.	1.7	16
48	Direct growth of MnCO3 on Ni foil for a highly sensitive nonenzymatic glucose sensor. Journal of Alloys and Compounds, 2018, 762, 216-221.	2.8	14
49	Ni Doping in MnO ₂ /MXene (Ti ₃ C ₂ T _{<i>x</i>}) Composites to Modulate the Oxygen Vacancies for Boosting Microwave Absorption. ACS Applied Electronic Materials, 2022, 4, 3694-3706.	2.0	13
50	Ternary MXene/MnO2/Ni composites for excellent electromagnetic absorption with tunable effective absorption bandwidth. Journal of Alloys and Compounds, 2022, 911, 165122.	2.8	12
51	In situ fabrication of Co(OH)2 by hydrothermal treating Co foil in MOH (M = H, Li, Na, K) for non-enzymatic glucose detection. Journal of Alloys and Compounds, 2019, 781, 1033-1039.	2.8	11
52	Effect of a coupling agent on the electromagnetic and mechanical properties of carbon black/acrylonitrile–butadiene–styrene composites. Journal of Applied Polymer Science, 2006, 102, 1839-1843.	1.3	9
53	β-MnO2 microrods for the degradation of methyl orange under acid condition from aqueous solutions. Research on Chemical Intermediates, 2017, 43, 3975-3987.	1.3	8
54	FACILE SYNTHESIS AND MICROWAVE ABSORPTION PROPERTIES OF α-MnO2 NANORODS. Functional Materials Letters, 2012, 05, 1250043.	0.7	7

#	Article	IF	CITATIONS
55	Combustion synthesized hierarchically porous Mn ₃ O ₄ for catalytic degradation of methyl orange. Canadian Journal of Chemical Engineering, 2017, 95, 643-647.	0.9	6
56	A nickel foam modified with electrodeposited cobalt and phosphor for amperometric determination of dopamine. Mikrochimica Acta, 2019, 186, 602.	2.5	6
57	NiO nanosheets on pine pollen-derived porous carbon: construction of interface to enhance microwave absorption. Journal of Materials Science: Materials in Electronics, 2020, , 1.	1.1	6
58	In situ fabrication of Ni(OH)2 nanoflakes/K-Ti-O nanowires on NiTi foil for high performance non-enzymatic hydrogen peroxide sensing. Journal of Electroanalytical Chemistry, 2019, 842, 107-114.	1.9	5
59	Ru-functionalized Ni-doped dual phases of $\hat{1}\pm \hat{1}^3$ -Fe2O3 nanosheets for an optimized acetone detection. Journal of Nanostructure in Chemistry, 2023, 13, 577-589.	5.3	4
60	1D Zn2GeO4 rods supported on Ni foam for high performance non-enzymatic hydrogen peroxide sensor. Surfaces and Interfaces, 2021, 25, 101295.	1.5	3
61	IN-SITU PREPARATION AND MAGNETIC PROPERTIES OF Fe ₃ O ₄ /WOOD COMPOSITE. , 2011, , .		1